Electronic Supplementary Material (ESI) for Catalysis Science & Technology.

Mechanistic insights into the conversion of polyalcohols over Brønsted acid sites

Quy P. Nguyen, Han K. Chau, Lance Lobban, Steven Crossley, Bin Wang*

School of Chemical, Biological and Materials Engineering, University of Oklahoma,

Norman, OK 73019, USA

Corresponding author's email: *wang_cbme@ou.edu

S1. Atomic models

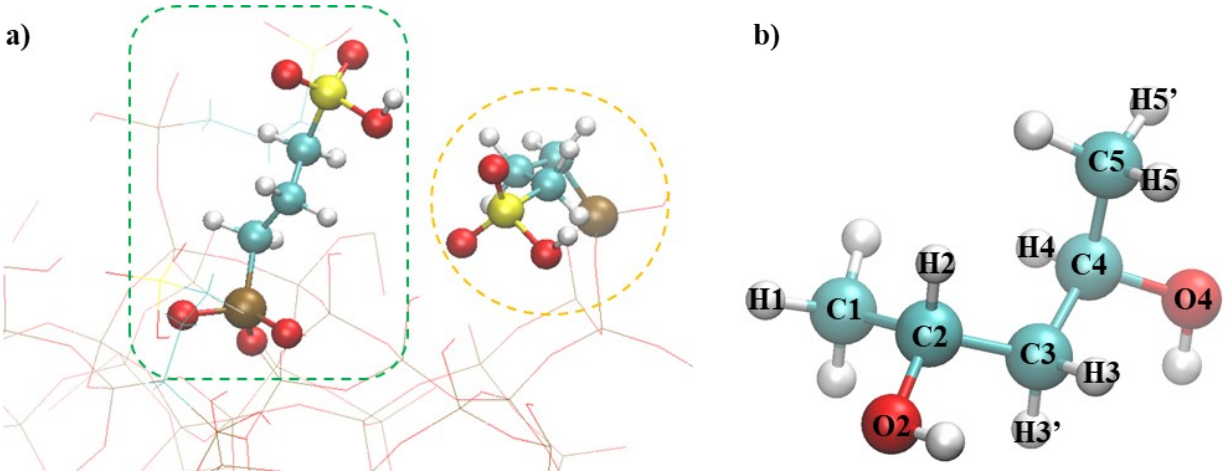

Figure S1. Atomic models: a) Amorphous silica functionalized with propylsulfonic groups. The structure was taken from one of our previous studies[1]. The sulfonic group in green box is the active site. The sulfonic group in orange circle is adjacent to the active site, where the water byproduct molecule adsorbs on during the first dehydration. The basic oxygen of the active site during the reaction of interest is named "Os"; **b)** Numbering of atoms in reactions. The OH group of O2 oxygen is firstly dehydrated.

S2. Statistical thermodynamics calculation

The entropy of a gas-phase molecule was computed based on the statistical thermodynamics[2] :

$$S_{gas-phase} = S_{trans} + S_{rot} + S_{vib}$$

Where: S_{trans}, S_{rot}, S_{vib} are, respectively, the translational, rotational, and vibrational entropies, which are calculated as follows.

$$S_{trans} = \mathrm{k}_B.\ln Q_{trans} + k_B T.\left[\frac{\partial ln(Q_{trans})}{\partial T}\right]_{N,V}$$

$$Q_{trans} = \frac{q_{trans}^{N}}{N!}$$

$$q_{trans} = \left(\frac{2\pi m k_B T}{h^2}\right)^{\frac{3}{2}}.V$$

$$S_{rot} = \mathrm{k}_B.\ln Q_{rot} + k_B T.\left[\frac{\partial ln(Q_{rot})}{\partial T}\right]_{N,V}$$

$$Q_{rot} = \frac{q_{rot}^{N}}{N!}$$

$$q_{rot} = \left(\frac{8\pi^2 k_B T}{h^2}\right)^{\frac{3}{2}}.\frac{\sqrt{\pi I_x I_y I_z}}{\sigma}$$

$$I_{x,y,z} = \sum_{i}^{number\ of\ atoms} m.d^{2}_{i-(x,y,z)\ axis}$$

$$S_{vib} = \mathrm{k}_B.\ln Q_{vib} + k_B T.\left[\frac{\partial ln(Q_{vib})}{\partial T}\right]_{N,V}$$

$$q_{vib-gas} = \prod_{i}^{3n-6} \frac{1}{1 - exp\left(\frac{-h\nu_i}{k_B T}\right)}$$

The entropic change of adsorption/ desorption is estimated:

$$\Delta S_{ads/\,des} = \frac{1}{3} S_{trans\ of\ gas-phase\ molecule}$$

The zero-point energy (ZPE), internal energy (U), enthalpy (H), Gibbs free energy (G) are calculated following the statistical thermodynamics.[2]

$$E_{ZPE} = \sum_{i}^{modes} \frac{1}{2} h\nu_i$$

$$U = E_{electronic\ (DFT-D3)} + E_{ZPVE} + k_B T^2 . \left[\frac{\partial ln\left(Q_{total\ ensemble}\right)}{\partial T}\right]_{N,V}$$

$$Q_{total\ ensemble} = \frac{\left(q_{trans} . q_{rot} . q_{vib}\right)^N}{N!}$$

For gas-phase species, the partitions $q_{trans} . q_{rot} . q_{vib}$ are computed as above.

For adsorbate/surface species, the ensemble is computed following:

$$Q_{total\ ensemble} = \frac{\left(q_{vib-adsobate}\right)^N}{N!}$$

$$q_{vib-adsorbate} = \prod_{i}^{3n} \frac{1}{1 - exp\left(\frac{-h\nu_i}{k_B T}\right)}$$

$$H = U + PV = U + RT$$

$$G = H - TS$$

$$S_{gas-phase} = S_{trans} + S_{rot} + S_{vib}$$

$$S_{adsorbate} = \mathrm{k}_B.\ln Q_{total\ ensemble} + k_B T.\left[\frac{\partial ln(Q_{total\ ensemble})}{\partial T}\right]_{N,V}$$

$$Q_{total\ ensemble} = \frac{(q_{vib-adsobate})^N}{N!}$$

$$q_{vib-adsorbate} = \prod_i^{3n} \frac{1}{1 - exp\left(\frac{-h\nu_i}{k_B T}\right)}$$

S3. Energetics of reaction at elementary steps

Table S1. Energetics of reaction at elementary steps. The energy differences are displayed in unit of kJ/mol for all, except the entropy displayed in J/mol/K.

Reaction	ΔE_{DFT+D3}	ΔE_{ZPVE}	ΔU	ΔH	ΔS	ΔG
1	-55.3	3.2	-45.6	-49.8	-58.5	-20.5
2	24.3	-2.2	26.1	26.1	17.1	17.6
3	47.3	-9.2	44.4	44.4	35.8	26.6
4	71.6	-11.4	70.6	70.6	52.9	44.1
5	42.0	-0.1	32.8	37.0	46.1	13.9
6	-48.6	0.6	-50.3	-50.3	-6.7	-47.0
7	31.3	-4.3	33.4	33.4	31.4	17.7
8	28.9	-8.1	25.0	25.0	35.3	7.4
9	33.7	-3.3	21.2	28.6	46.1	5.6
10	36.9	-2.4	27.8	32.0	56.8	3.6

11	-15.4	-1.2	-16.4	-16.4	10.6	-21.7
12	-32.6	10.9	-28.5	-28.5	-51.1	-2.9
13	33.2	-10.0	28.9	28.9	43.7	7.1
14	40.5	-0.9	33.0	37.1	57.9	8.2
15	-34.1	10.0	-29.8	-29.8	-37.3	-11.1
16	-16.9	-0.6	-17.4	-17.4	-3.2	-15.8
17	-45.2	-7.6	-50.5	-50.5	29.0	-65.0
18	55.6	-2.9	46.2	50.4	57.7	21.5

S4. Energetics of intrinsic activation barriers at elementary steps

Table S2. Energetics of intrinsic activation barrier at elementary steps. The energy differences are displayed in unit of kJ/mol for all, except the entropy displayed in J/mol/K.

Transition state	ΔE_{DFT+D3}	ΔE_{ZPVE}	ΔU	ΔH	ΔS	ΔG
TS1	171.7	-15.7	162.2	162.2	25.3	149.6
TS2	137.6	-15.0	125.4	125.4	14.5	118.2
TS3	161.9	-17.5	148.7	148.7	14.0	141.7
TS4	104.6	-3.9	100.2	100.2	-18.9	109.7
TS5	80.7	-12.8	68.5	68.5	5.3	65.8
TS6	110.8	-6.1	101.0	101.0	-32.5	117.2
TS7	168.9	-16.5	155.8	155.8	24.5	143.6
TS8	166.5	-7.0	158.6	158.6	-16.4	166.8
TS9	180.7	-9.5	172.6	172.6	14.6	165.3
TS10	65.1	-6.2	60.7	60.7	4.3	58.5

S5. Optimized structures in the first dehydration

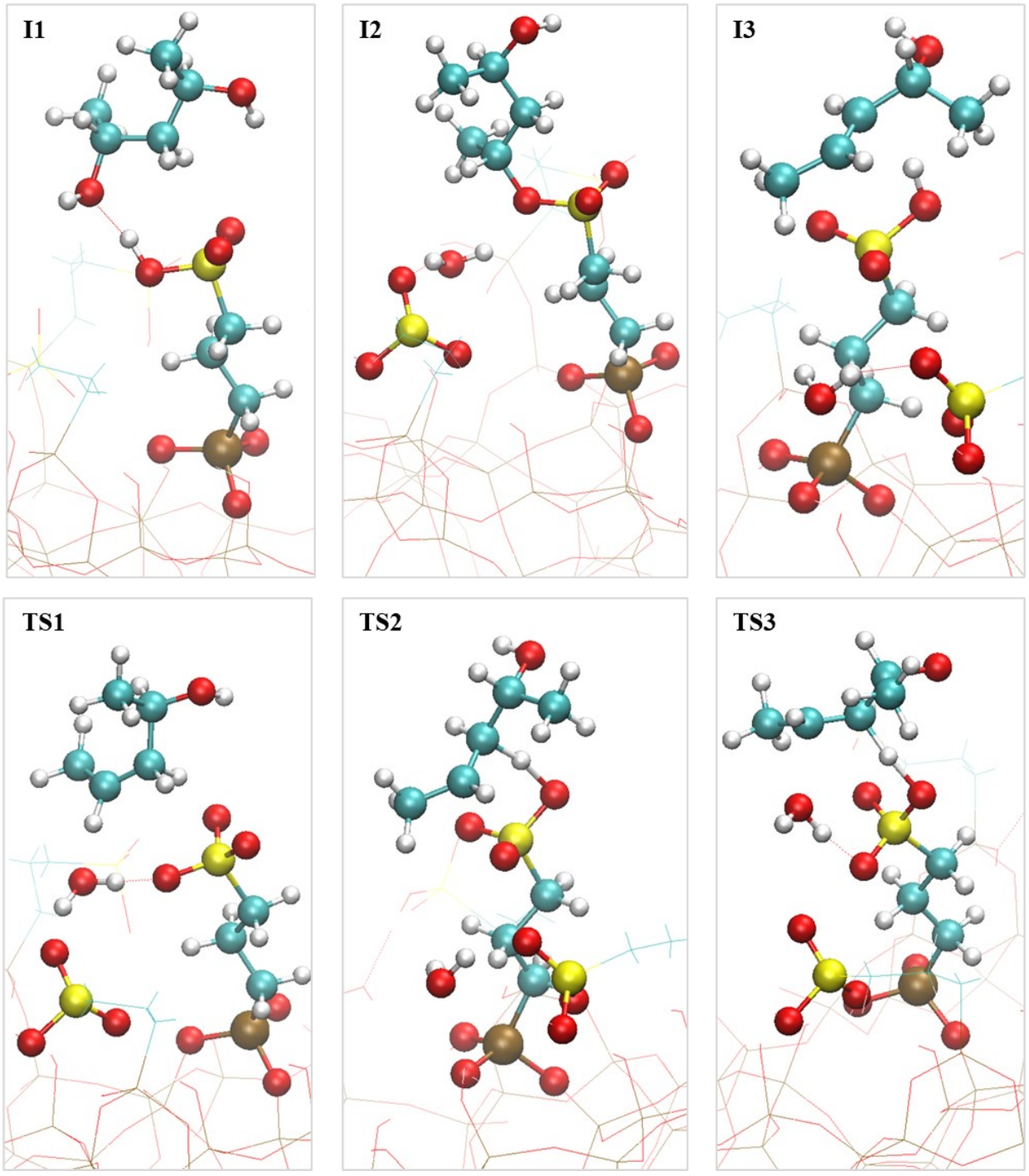

Figure S2. Optimized structures in the first dehydration. The structure is named following the corresponding states in Figure 3. The structure of I4 is the same as I3, except the water molecule desorbed from the adjacent sulfonic group.

S6. Optimized structures in the second dehydration

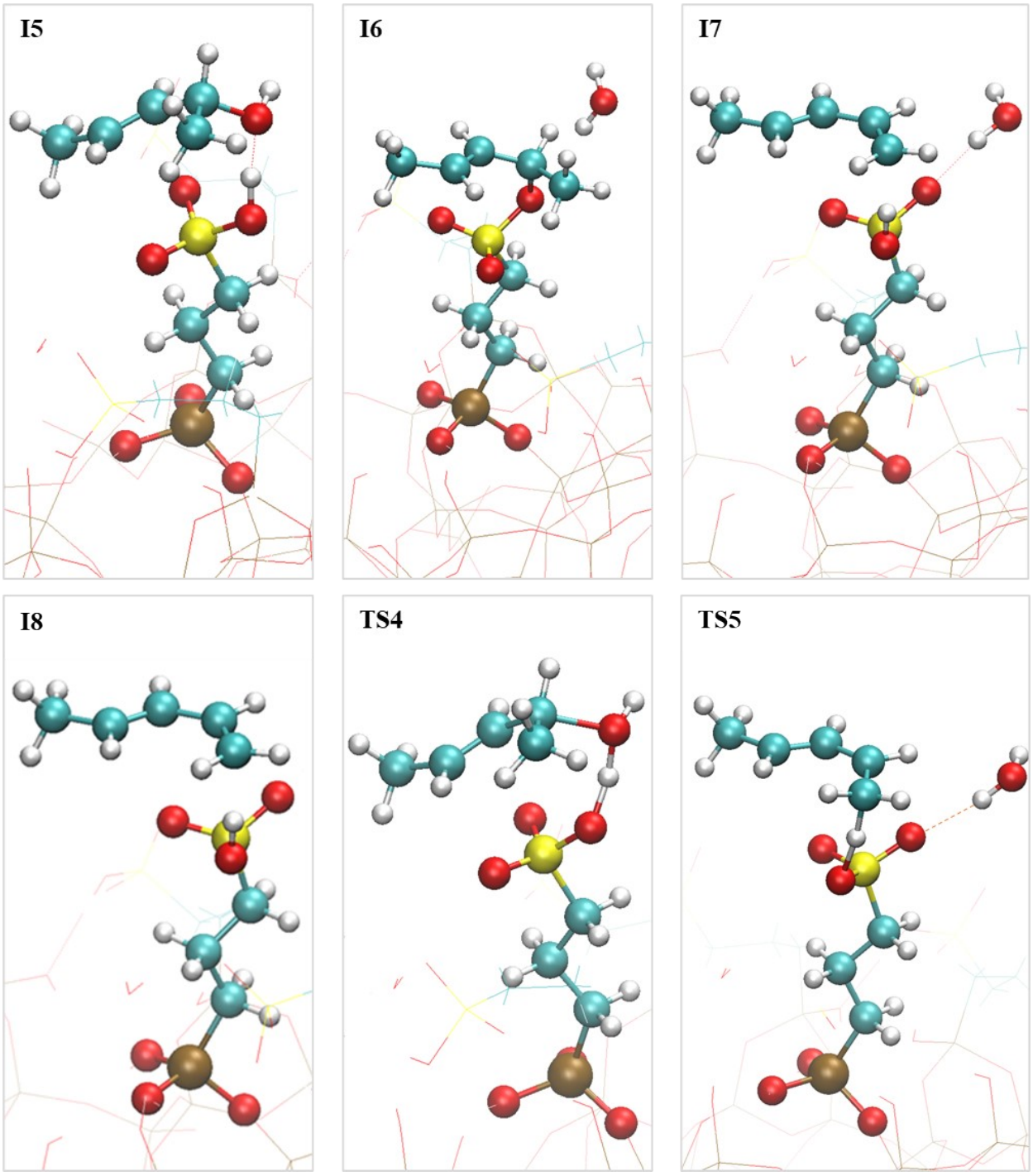

Figure S3. Optimized structures in the second dehydration. The structure is named following the corresponding states in Figure 4.

S7. Optimized structures in the C=C bond migration

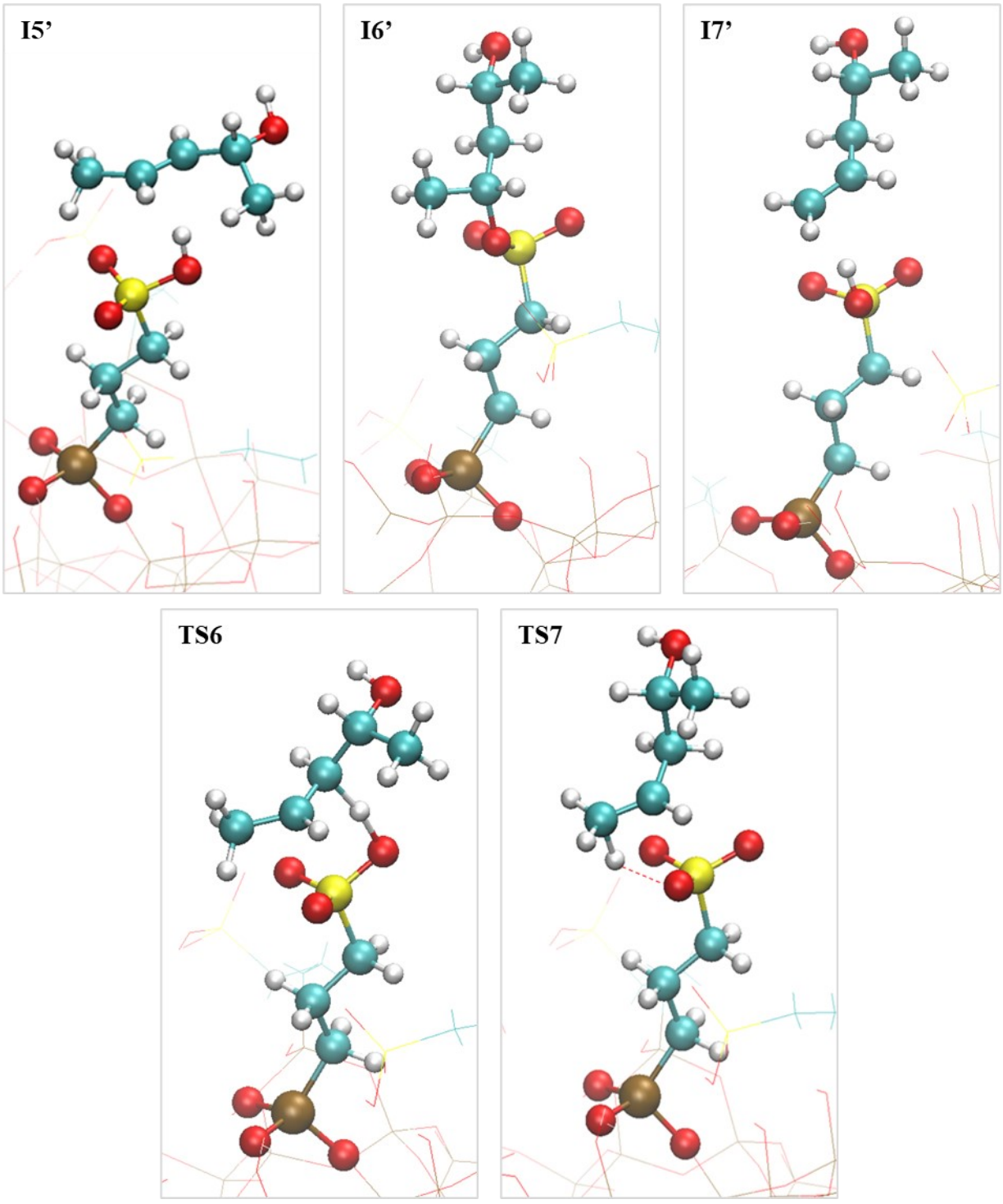

Figure S4. Optimized structures in the C=C bond migration. The structure is named following the corresponding states in Figure 4.

S8. Optimized structures in the ketone formation

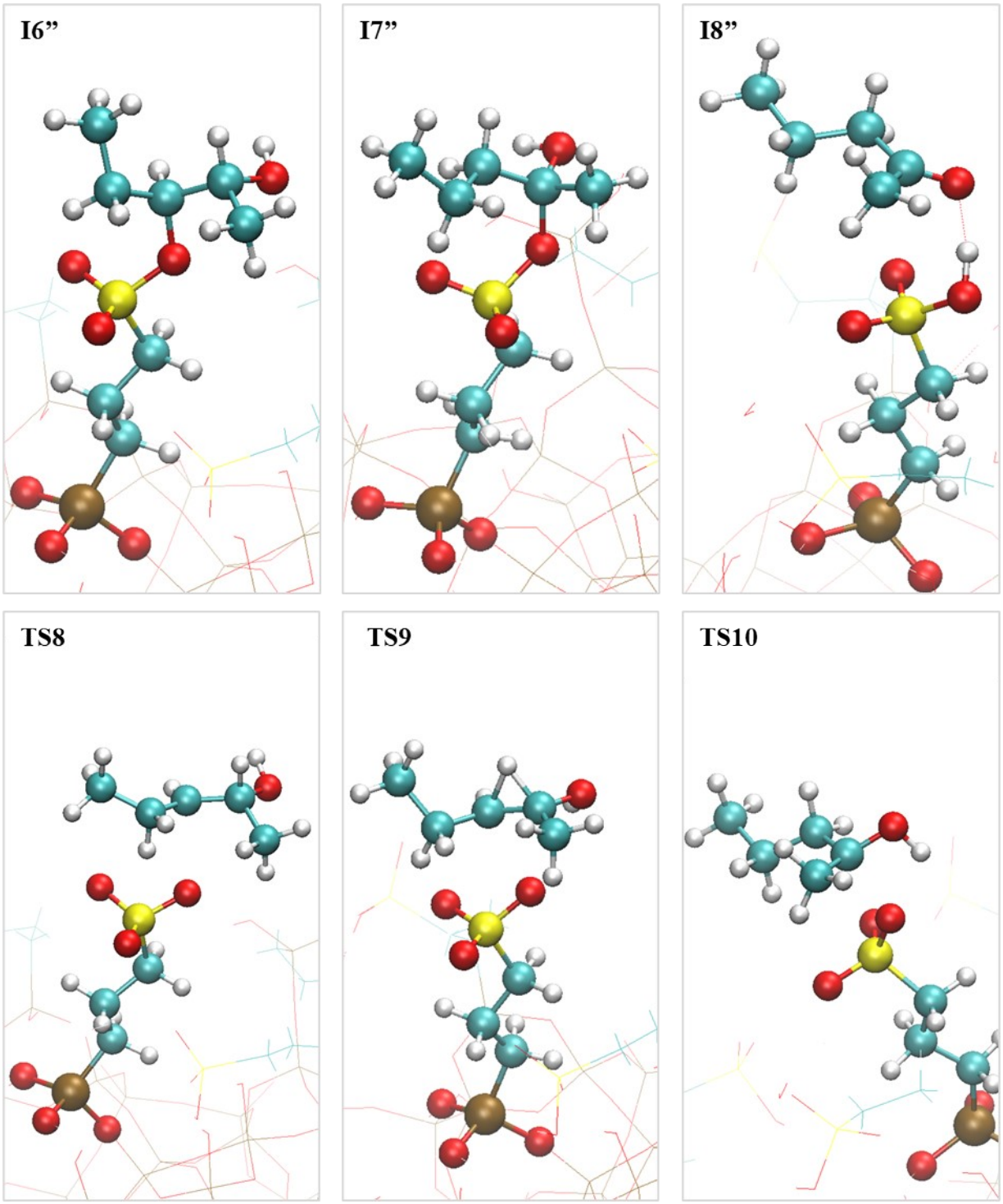

Figure S5. Optimized structures in the ketone formation. The structure is named following the corresponding states in Figure 4. The structure of I5’ is shown in Figure S4.

S9. Computation of theoretical apparent activation barriers

Table S3. Degrees of rate-control of surface species and transition states during pathways of three different secondary products. The orange, blue, and green tables are, respectively, of the diene formation, the C=C bond migration, and the ketone formation. The calculation follows the energetic span model[3] for each separate pathways. The name of states is referred to Figure 4.

Surface species	Degree of Rate-control
I1	3%
I3	0%
I4	0%
I5	96%
I6	1%
I7	0%
I8	0%

Transition State	Degree of Rate-control
TS3	100%
TS4	0%
TS5	0%

Surface species	Degree of Rate-control
I1	99%
I3	0%
I4	0%
I5'	0%
I6'	1%
I7'	0%

Transition state	Degree of Rate-control
TS3	0%
TS6	1%
TS7	99%

Surface species	Degree of Rate-control
I1	45%
I3	0%
I4	0%
I5''	0%
I6''	0%
I7''	0%
I8''	55%

Transition state	Degree of Rate-control
TS3	0%
TS8	95%
TS9	5%
TS10	0%

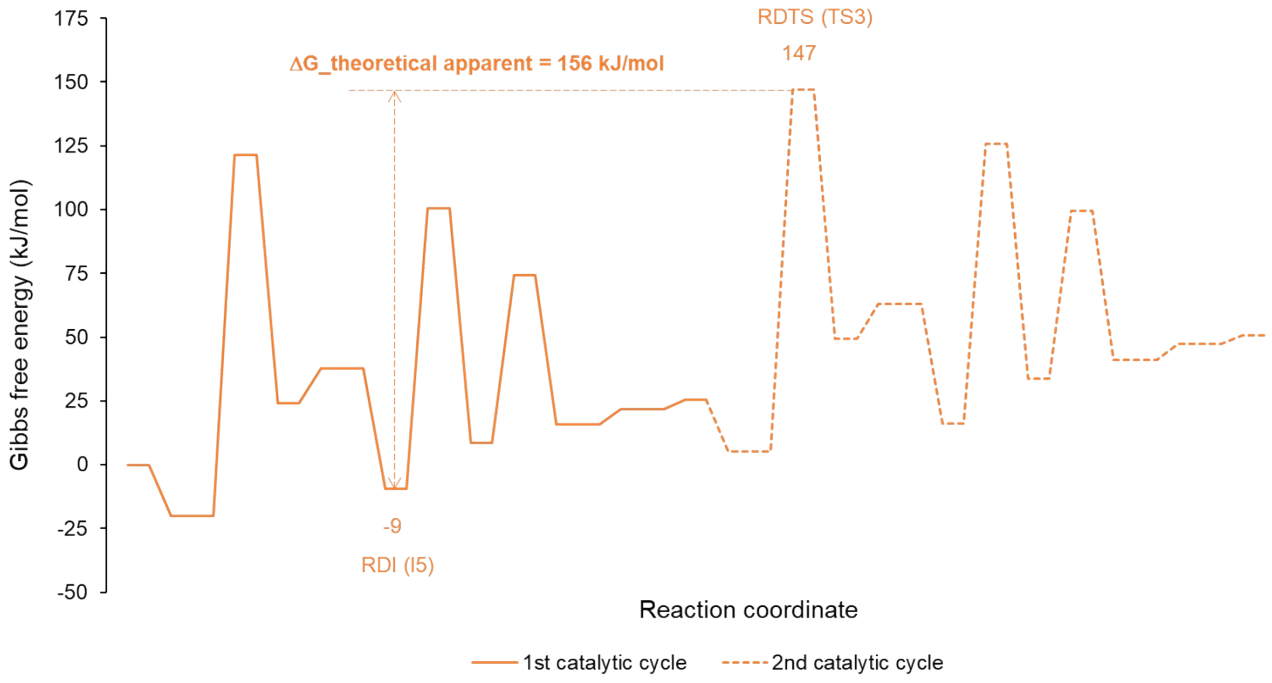

Figure S6. The RDI and RDTS during the pathway of dienes formation.

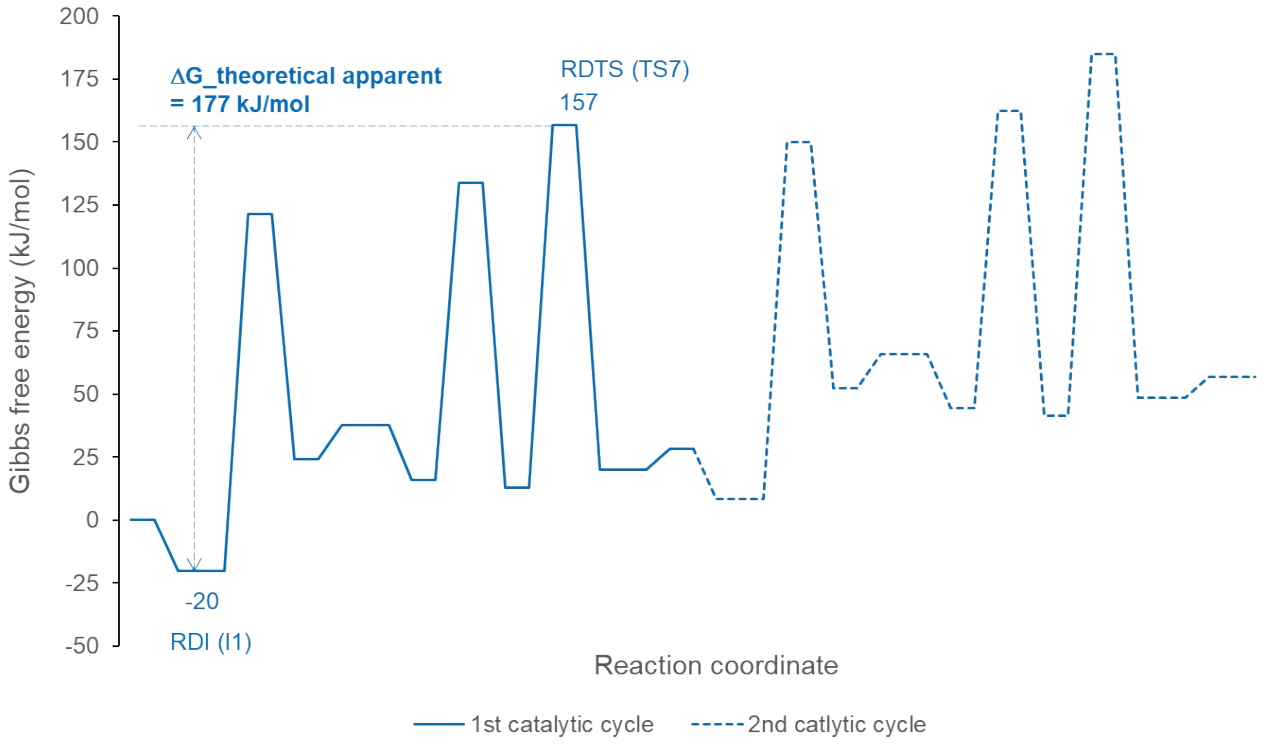

Figure S7. The RDI and RDTS during the pathway of C=C bond migration.

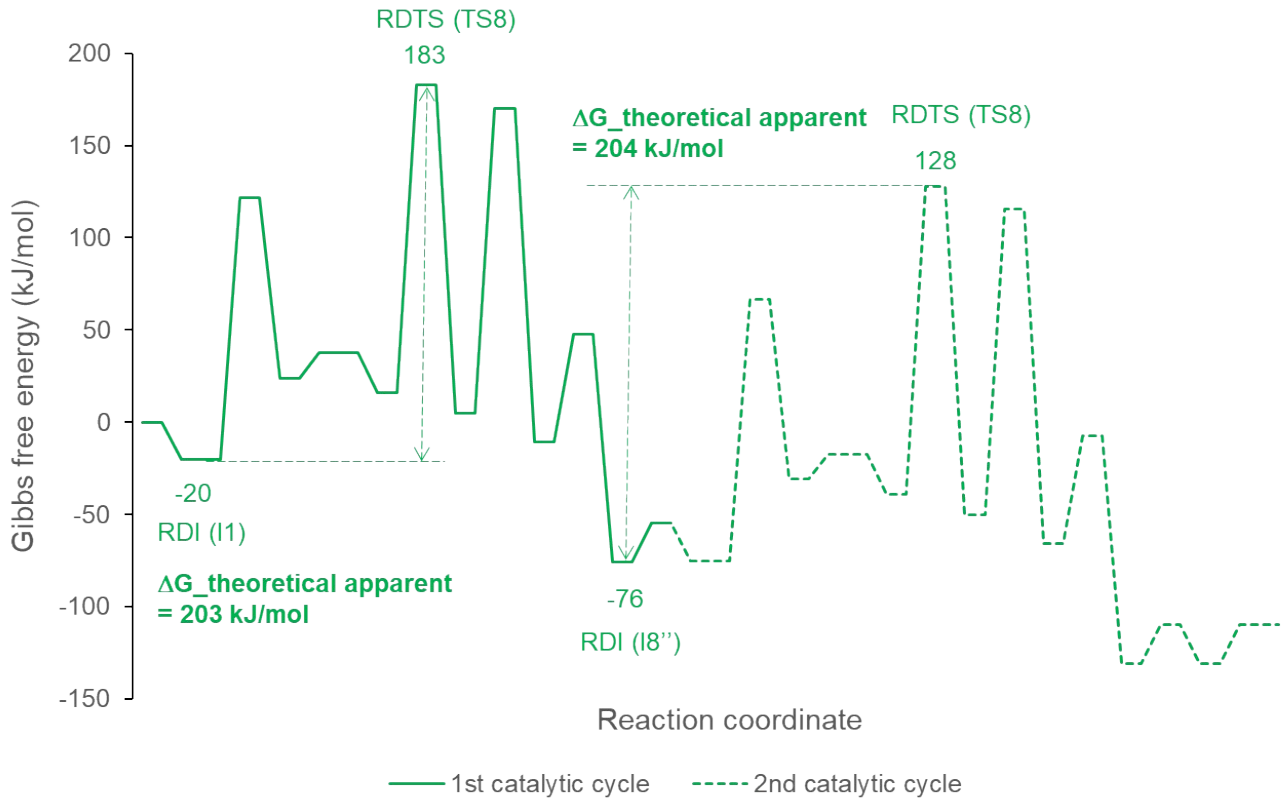

Figure S8. The RDI and RDTS during the pathway of ketone formation.

S10. Catalyst preparation and characterization

2,4-pentanediol (98%), silica gel (high-purity grade, Davisil Grade 646, 35-60 mesh, pore size 150 Å), 3-mercaptopropyl trimethoxysilane (MPTMS, 95%), anhydrous methanol (99.8%), anhydrous ethanol (≥99.5%), hydrogen peroxide aqueous solution (30 wt.%) were purchased from Sigma-Aldrich and used as received.

Sulfonic acid-functionalized silica was prepared by high-temperature grafting silylation method to minimize leaching of acid functional group from the silica support in liquid phase reaction.[1, 4] Before functionalization, the silica gel was dried overnight at 80°C in a vacuum oven

to remove any physiosorbed water. Incipient wetness impregnation was carried out by adding dropwise 3.45 ml of methanol solution of 2.5 M 3-mercaptopropyl trimethoxysilane onto 2.89 g of silica gel. The solid was transferred to a Teflon-lined autoclave and heated to 180°C for 14 h. After functionalization, the solid was washed three times with ethanol and dried at 80°C in a vacuum oven for 12 h. The sample was oxidized in 25 mL of a 30 wt.% H_2O_2 stirred solution at room temperature for 12 h to obtain the sulfonic acid groups. The solid was separated from the solution, washed three times with ethanol, and dried at 80°C in a vacuum oven for 12 h. The acid-functionalized silica catalyst is denoted as SiO_2-SO_3H.

Thermogravimetric analysis with the temperature program oxidation (TGA-TPO) was performed on a Netzsch STA 449F1 equipped with a pin thermocouple and a Netzsch nano-balance to quantify the number of functional groups per gram catalyst. The catalyst sample was placed in a crucible with a constant flow of argon (20 ml/min) and air (40 ml/min). The cell was preheated to 40°C for 10 min before being increased to 700°C with a ramping rate of 3°C/min. The outlet gases (H_2O, CO_2, SO_2) were analyzed on an on-line mass chromatography Aeolos QMS 403C.

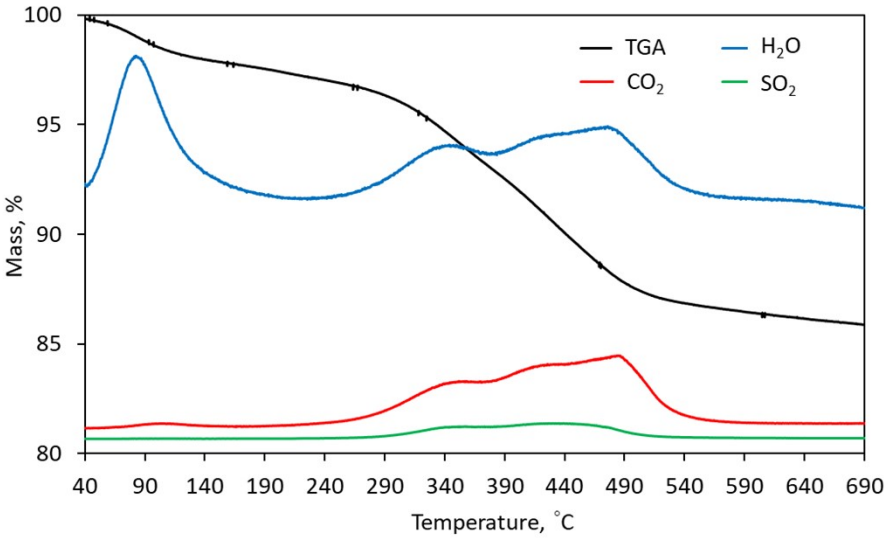

Figure S9. TGA-TPO plot of the SiO_2-SO_3H catalyst.

Figure S9 shows the TGA-TPO result of the SiO_2-SO_3H catalyst with four temperature regions consistent with the previous report.[4] The mass loss in the temperature range of 40-120°C is attributed to the removal of physiosorbed water, as indicated by the peak of water in the mass spectrometry. There is no significant mass loss and detectable MS peaks in the second temperature region (120-300°C). The third temperature range of 300-500°C shows a considerable mass loss due to the thermal degradation of the functional groups, as MS peaks of CO_2, SO_2, and H_2O were detected. Based on the mass loss in this region, the acid site density of the sulfonic acid-functionalized silica was obtained with 0.902 mmol/g sulfonic groups per gram catalyst. The small mass loss in the temperature above 500°C is attributed to the thermal dehydroxylation[5] of free silanol groups on the catalyst surface. Therefore, it is expected that there would be no catalyst structural change after the pretreatment at 250°C and the reaction at 200°C.

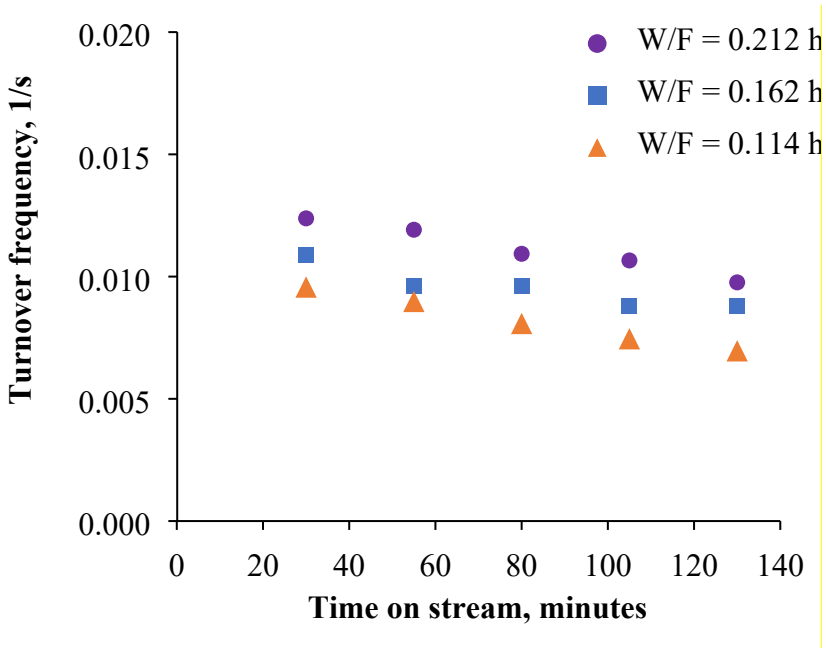

Figure S10. Turnover frequency measured as a function of time on stream at different W/F.

The stability of the catalyst during the reaction time on stream with varying reaction space time is shown in Fig. S10. From 30 minutes to 130 minutes time on stream, the reaction turnover frequency drops about 20% for the higher reaction space time or conversion (W/F = 0.212 h and 0.162 h), whereas the reaction turnover frequency decreases about 27% for the lower reaction space time or conversion (W/F = 0.114 h). While the difference in the catalyst stability with varying reaction space time is marginal, the more stable catalyst in the case of higher conversion may indicate that the catalyst deactivation is not simply due to the oligomerization of the major product, i.e., pentadiene.

Table S4. Experimentally measured chemical reaction rates of 2,4-pentanediol dehydration per catalyst mass base and per active site base.

W/F	Conversion, %	Reaction rate, mol/g_{cat}.s	Turnover frequency, 1/s
0.114	40.7%	0.0106	9.57×10^{-6}
0.162	61.4%	0.0112	1.01×10^{-5}
0.212	95.6%	0.0134	1.21×10^{-5}

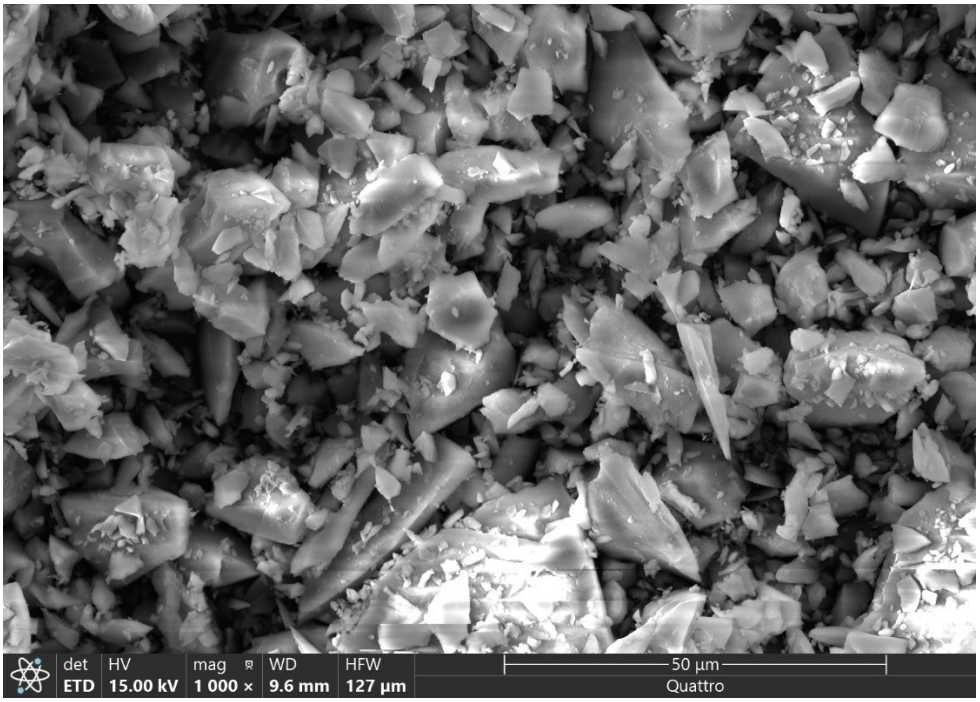

Figure S11. SEM image of the SiO_2-SO_3H catalyst.

The effect of external mass diffusion on the dehydration of 2,4-pentanediol over the SiO_2-SO_3H catalyst has been investigated by using the Mears criterion which is the ratio of measured chemical reaction rate to the external mass diffusion rate.[6] The effect of external mass diffusion can be neglected if the Mears criterion is less than 0.15.

$$\frac{-r_A^{'}\rho_b Rn}{k_c C_{Ab}} < 0.15$$

where $r_A^{'}$ = reaction rate per unit mass of catalyst (kmol/kg_{cat}.s), n = reaction order, R = catalyst particle radius (m), ρ_b = bulk density of the catalyst bed (kg/m^3), $\rho_b = (1-\varepsilon)\rho_c$, ε = catalyst bed porosity, ρ_c = catalyst density, C_{Ab} = bulk concentration of the reactant (kmol/m^3), and k_c = external mass transfer coefficient (m/s).

The particle radius of the catalyst is estimated based on the SEM image analysis. The external mass transfer coefficient is calculated according to the Thoenes- Kramers correlation.[7] The binary gas-phase diffusion coefficient is estimated by using the proposed empirical correlation.[8] As the partial pressure of the reactant is 0.3 kPa, the fluid density and viscosity are obtained by using the pure helium gas. In the extreme case, i.e., at a high measured chemical reaction rate and large particle radius with 95% confidence interval, the Mears criterion is still less than 10^{-3}. This evaluation has proved that the reaction is not limited by external mass diffusion.

References

1. G. Li, B. Wang, B. Chen and D. E. Resasco, *Journal of Catalysis*, 2019, **377**, 245-254.
2. C. J. Cramer, *Essentials of computational chemistry: theories and models. John Wiley & Sons, 2004.*.
3. S. Kozuch and S. Shaik, *Accounts of Chemical Research*, 2011, **44**, 101-110.
4. T. V. Bui, S. J. Umbarila, B. Wang, T. Sooknoi, G. Li, B. Chen and D. E. Resasco, *Langmuir*, 2019, **35**, 6838-6852.
5. X. S. Zhao, G. Lu, A. Whittaker, G. Millar and H. Zhu, *The Journal of Physical Chemistry B*, 1997, **101**, 6525-6531.
6. D. E. Mears, *Ind. Eng. Chem. Process Des. Dev.* 1971, **10**, 4, 541–547
7. S. H. Fogler, Elements of Chemical Reaction Engineering, Pearson, 5th edition, 2016
8. E. N. Fuller, P. D. Schettler, and J. C. Giddings, *Ind. Eng. Chem.* 1966, **58**, 5, 18–27